# CHAPTER II
# THEORETICAL BACKGROUND AND LITERATURE REVIEWS

## 2.1 Artificial Muscle as an Actuator

Various natural muscles are incredibly efficient material systems that allow large deformations by repetitive molecular motions. Polymer artificial muscle technologies are being developed that are expected to produce high strains and high stresses through electrostatic force, electrostriction, ion insertion, and molecular conformational changes. There are presently a variety of polymers that exhibit substantial deformations in response to an applied voltage. These materials reversibly contact and expand in length and volume, and they are called actuators, similar to living muscles. It is interesting to compare the performance characteristics of polymer artificial muscles with natural muscles in terms of utilization respond rate, elastic modulus, strain, stress, and etc. The applications of muscle-like materials are in medical devices, prostheses, robotics, toys, biomimetic devices (Baughman, 1996; Mirfakhrai *et al.*, 2007). Figure 2.1 shows three states during the electromechanical cycle of a rocking-chair-type, a bimorph actuator. Both electrodes have the same concentration of a dopant ($K^+$) when the cantilever is undistorted, and electrochemical transfer of the dopant between electrodes causes bending either to the right or to the left (Baughman *et al.*, 1996).

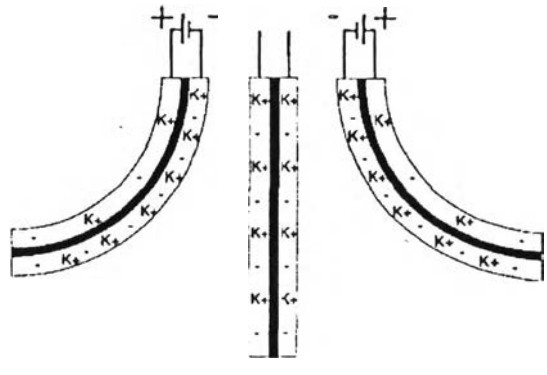

**Figure 2.1** Schematic representative of three states during the electromechanical cycle of a rocking-chair-type, bimorph actuator (Baughman *et al.*, 1996).

Palakodeti *et al.* (2006) studied the effects of frequency and bidirectional static pre-strain of acrylic elastomer films. The viscoelastic mechanical properties of the elastomeric acrylic films were analyzed by the dynamic mechanical analysis to determine the mechanical efficiency of the actuators. The pre-strained elastomer films were used as an electroactive polymer actuator, sometimes referred to as artificial muscles, where the loss tangent determined the mechanical efficiency of the actuator. The acrylic elastomers, with glass transition temperature of approximately -40°C, were tested in the rubbery region and the experiments were set up as shown in Figure 2.2. The result showed that mechanical efficiency of the actuator increased with increasing bidirectional prestrain, and decreased with increasing frequency.

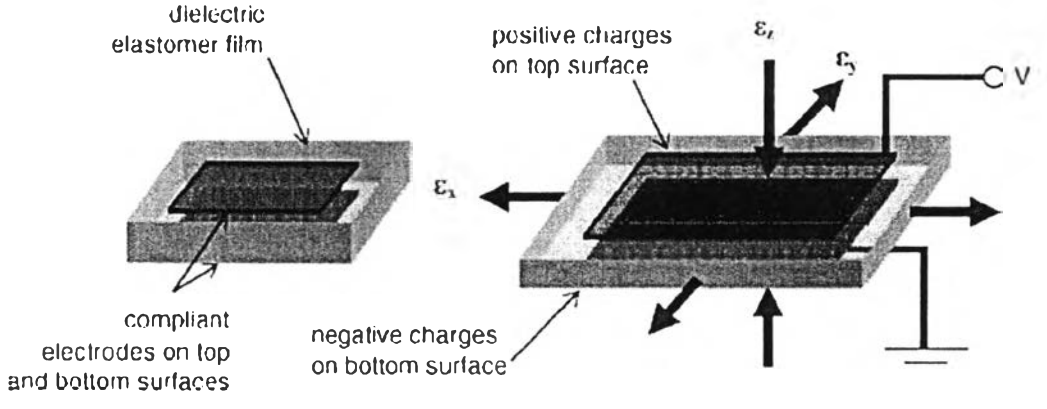


**Figure 2.2** Electroactive polymer actuation (Palakodeti *et al.*, 2006).

Kunchornsup *et al.* (2012) studied cross-linked cellulosic gels (Phy_gel), which were prepared by the solvent casting method using 1-butyl-3-methylimidazolium chloride ionic liquid to dissolve microcrystalline celluloses. The relative dielectric permittivity increased with increasing frequency because of the ionic polarization. The effect of temperature on the relatively dielectric permittivity was linearly related at relative low temperature due to the temperature induced ion mobility and polarization. At a relative high temperature, the effect of temperature on relative permittivity was inversely proportional because of the ionic association. The electric field strength induced the internal dipole moments at a relatively low temperature, and the storage modulus increased. The deflection experiment in Figure

2.3 showed the bending towards the positive side under electric field strength above 100 V/mm.

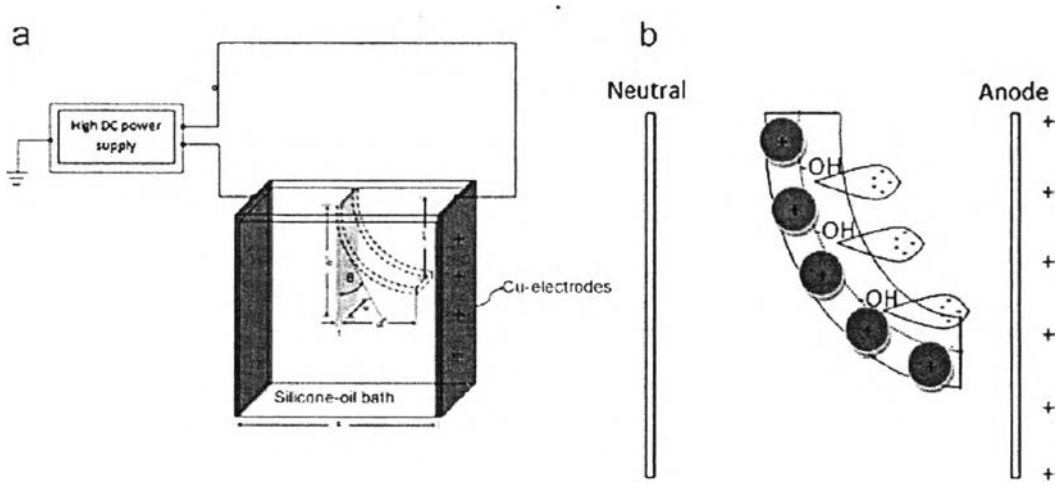


**Figure 2.3** Schematic illustrations of: (a) bending response measurement of Phy gel suspended vertically in silicone-oil bath and sandwiched between copper electrodes. A DC electric field was applied horizontally at 30 ± 0.5°C causing a deflection distance; (b) actuation mechanisms were from two dominating factors; ionic polarization of BMIM+ cation and electronic polarization of cellulosic hydroxyl group.

Shahinpoor (2003) summarized the fundamental properties and characterized the ionic polymeric-conductor composites (IPCCs) as biomimetic sensors, robotic actuators, and artificial muscles. In particular, the manufacturing techniques were discussed including a comparison between chemical plating and physical loading of a conductor phase, the electronic and electromechanical characteristics of IPCCs, the phenomenological modeling of the underlying sensing and actuation mechanisms in IPCCs, some preliminary constitutive modeling of such complex electroactive materials, as well as some potential industrial and medical application areas for IPCCs, respectively. It also briefly discussed the potential of IPCCs in developing distributed biomimetic micro and nano sensors and actuators.

Cianchetti *et al.*, (2009) studied a new soft actuator based on electroactive polymers (EAPs) technology. The actuator was composed of a pre-stretched silicone

film sputtered with a very thin gold film on both sides, working as electrodes. A particular folded geometry, implemented through an innovative fabrication process, allowed the exploitation of the electrostrictive effect and to develop soft actuators suitable in many applications where softness and flexibility are necessary. The manufactured prototypes were developed on the basis of a parametric model that took into account all geometric parameters and material characteristics. The proposed model was useful to estimate the performances of the actuator and to improve them.

## 2.2 Electroactive Polymers (EAPs)

Since the early 90s, electroactive polymers have emerged that can be stimulated to produce a significant shape or size change. The similar behavior of these materials to biological muscles acquired them the name "artificial muscles". Generally, there are many polymers that exhibit a volume or shape change in response to perturbation of the balance between repulsive intermolecular forces, which act to expand the polymer network, and attractive forces which act to shrink it. Repulsive forces are usually electrostatic or hydrophobic in nature, whereas attraction is mediated by hydrogen bonding or van der Waals interactions. The competition between these counteracting forces, and hence the volume or shape change, can be controlled by subtle changes in parameters such as solvent, gel composition, temperature, pH, light, and etc. (Bar-Cohen, 2002 and 2004).

Electroactive polymers (EAPs) are the polymers that exhibit a shape change in response to electrical stimulation which can be divided into two distinct groups: electronic EAPs and ionic EAPs. Electronic EAPs are very attractive in performing the energy conversion between the electric and mechanical forms and hence can be utilized as both solid-state electromechanical actuators and motion sensors. The electromechanical response of this polymer can be linear such as in typical piezoelectric polymers or non-linear such as the electrostrictive polymers and Maxwell stress effect induced response. Whereas, ionic EAPs are driven by diffusion of ions and they require an electrolyte for the actuation mechanism. The examples of ionic EAPs are gels, polymer-metal composites, conductive polymers, and carbon nanotubes (Bar-Cohen, 2004; Shahinpoor *et al.*, 2007).

The following literature reviews are the examples of electroactive polymers and their applications;

Prissanaroon *et al.* (2000) studied the effects of dodecylbenzene sulfonic acid (DBSA) as a dopant on electrical conductivity of polypyrrole films in $N_2$ and $SO_2$ atmosphere. The polypyrrole films doped with DBSA can be used to detect small amount of $SO_2$. The short-time conductivity response of the conductive films can be improved by higher doping levels or by exposure to higher $SO_2$ concentrations. However, below a critical doping level, the gas sensitivity was independent of the doping level. Above the critical doping level, the gas sensitivity raised to a maximum and then slightly decreased as the dopant concentration was increased, which can be interpreted to be due to the changes in the conductive film morphology from three-dimensional random coils to rod-like fibrillar structure.

Hiamtup *et al.* (2006) synthesized polyaniline (PANI) via the oxidative coupling polymerization in an acid condition and de-doped in a solution of ammonia. The electrorheological (ER) properties of PANI/silicone oil suspensions were studied in oscillatory shear in the linear viscoelastic regime as functions of electric field strength, particle concentration, and host fluid viscosity. They also investigated the switching characteristics of the ER response and confirmed the existence of residual gel structure when the field was switched off, if the applied stress was too small. The results showed that when the field was switched off a residual structure remained, where yield stress increased with the strength of the applied field and particle concentration. When the applied stress exceeded the yield stress of the residual structure, a fast and fully reversible switching of the ER response was obtained.

Wichiansee *et al.* (2009) synthesized poly(3,4-ethylenedioxy thiophene)/ poly(stylene sulfonic acid) (PEDOT/PSS) via the chemical oxidative polymerization and mixed with ethylene glycol (EG) to improve the electrical conductivity. Furthermore, the PEDOT/PSS/EG particles were used for studying the electrorheological properties by blending with poly(dimethylsiloxane) (PDMS) as potential actuator materials. The results showed that EG particles became polarized and induced dipole moments were generated, leading to intermolecular interactions along the direction of electric field. Moreover, adding EG increased the particle electrical conductivity by more than an order of the magnitude through the

conformational change of the PEDOT chains from the random coil structure to the expanded expanded-coil structure and affected the electrorheological properties of PEDOT/PSS blends.

Chansai *et al.* (2009) prepared a conductive polymer hydrogel blended between sulfosalicylic acid doped polypyrrol (PPy) and poly(acrylic acid) (PAA) and used as a carrier/matrix for the transdermal drug delivery under applied electric field. PAA films and the blended films were prepared by solution casting with ethylene glycol dimethacrylate (EGDMA) as a cross-linking agent. The effect of cross-linking ratio and electric field strength on the diffusion of the drug from PAA and PPy/PAA hydrogels were studied. The diffusion coefficient became larger by an order of magnitude relative to those samples without electric field due to the electrostatic force from electrical potential driving the charged drug to the oppositely charged electrode. It can be concluded that, by varying the cross-linking density, the electric field strength, the drug size, the hydrogel matrix mesh size, the drug-matrix interaction, and the presence of a conductive polymer, the drug release can be controlled towards a desired level.

Tungkavet *et al.* (2012) fabricated nanowire-polypyrrole/gelatin hydrogel by solvent casting. The storage modulus sensitivity became high only at suitable nanowire-Ppy concentrations. However, the storage modulus response and sensitivity decreased with nanowire- Ppy concentration greater than 0.1 %v/v. For the hydrogel system with the highest particle concentration of 1.0 %v/v, the storage modulus response under the effect of the electric field was diminished since the hydrogel presumably involved a phase separation between the gelatin hydrogel and the nanowire-Ppy agglomeration. In the temporal response, the nanowire-Ppy/gelatin hydrogel (0.1 % v/v and 1.0 %v/v) showed that the storage modulus decreased when removing the applied electric field but they did not recover its original value. This behavior indicates that there were some irreversible agglomerations of the nanowire-Ppy or some dipole moment residues, possibly due to some hydrogen bonding between adjacent nanowire-Ppy. However, the 1.0% v/v of nanowire-Ppy/gelatin hydrogel exhibited a quick response under an electric field since the agglomeration of nanowire-Ppy in hydrogels constituted large induced dipole moment domains.

**Table 2.1** Comparison of the storage modulus sensitivity of dielectric elastomer and its composites under electric field strength of 2 kV/mm at 300 K

| Materials | Storage Modulus Sensitivity | Reference |
|---|---|---|
| Acrylic elastomer 70 | 0.439 | Kunanuruksapong *et al.*, 2007 |
| Acrylic elastomer 71 | 0.586 | |
| Acrylic elastomer 72 | 0.148 | |
| Styrene-acrylic copolymers | 1.195 | |
| Styrene-isoprene-styrene triblock | 0.746 | |
| Acrylic elastomer 71 + 10%v/v PPP | 0.306 | |
| Acrylic elastomer 71 + 30%v/v PPP | 0.971 | |
| Polyisoprene + 5%v/v Polythiopene | 0.523 | Thongsak *et al.*, 2010 |
| Polyisoprene + 10%v/v Polythiopene | 0.33 | |
| Polyisoprene + 30%v/v Polythiopene | 0.435 | |
| AR71+ 0.000019 %v/v lead zirconate titanate | 0.149 | Tangboriboon *et al.*, 2009 |
| AR71+ 0.038%v/v lead zirconate titanate | 0.587 | |
| Poly (dimethyl siloxane) | 0.104 | Hiamtup *et al.*, 2006 |
| Poly (dimethyl siloxane) + 20% v/v PANi | 0.25 | |
| Poly (dimethyl siloxane) + 2% v/v PANi | 0.111 | |
| PDMS + 5%v/v PEDOT/PSS/EG | 0.077 | Wichiansee *et al.*, 2009 |
| PDMS + 15%v/v PEDOT/PSS/EG | 0.333 | |

## 2.3 Conductive Polymers

Harun (2007) synthesized conjugated conducting polyacetylene when monomers of acetylene was doped with iodine and bromine vapor. The result was that electrical conductivity became higher 10 times than the undoped monomers. Due to the alternating single and double bonds in the polymer chain, called conjugated polymer, they enable the electrons to delocalize through the whole system and thus many atoms may share them. The delocalized electrons may move around the whole system and become the charge carriers making them conductive. This polymer can be transformed into a conducting form when electrons are removed from the backbone. Thus, anions and cations act as charge carriers, hopping from one site to another under the influence of an electric field to increase the conductivity (Harun, 2007).

There are examples of conductive polymers based on different aromatic monomers such as pyrrole, thiophene, aniline, azulene, carbazole, and etc. along with their derivatives have been studied towards improvements of both properties and applications (Bar-Cohen, 2004).

Because of the large energy separation (more than 3 eV) between the valence band and the conduction band, it is necessary to subject the polymers to a transformation process called "doping" to get their conductive states. It can be inferred that doping process can convert a conventional insulating polymer to a conducting polymer with near metallic conductivity. The doping process in conductive polymers can be carried out either chemically (through the employment oxidizing or reducing agents) or electrochemically. Thus, the unique feature of conducting polymers is that they combine the properties of two classes of materials: plastics and metals. The potential result is a material with the chemical and mechanical attributes of polymers and the electronic properties of metals or semiconductors (Bar-Cohen, 2004).

- N-doping: partial reduction of the neutral polymer chains to generate polyanions and simultaneous insertion of compensating cations to neutralize the negative charges created in the polymers.

- P-doping: partial oxidation of the neutral polymer chains to generate polycations and simultaneous insertion of compensating anions to neutralize the positive charges created in the polymers.

In the case of polyacetylene, as shown in Figure 2.4, when polarons and bipolarons are produced along the doping process, the cations are not bound to each other and can freely separate along the polymer chain causing solitons. Soliton formation results in the creation of new localized electronic states that appear in the middle of the energy gap. At high dopant levels, the charged solitons interact with other to form a soliton band which can be eventually merged with the conduction band to create true metallic conductivity (Pratt, 1996).

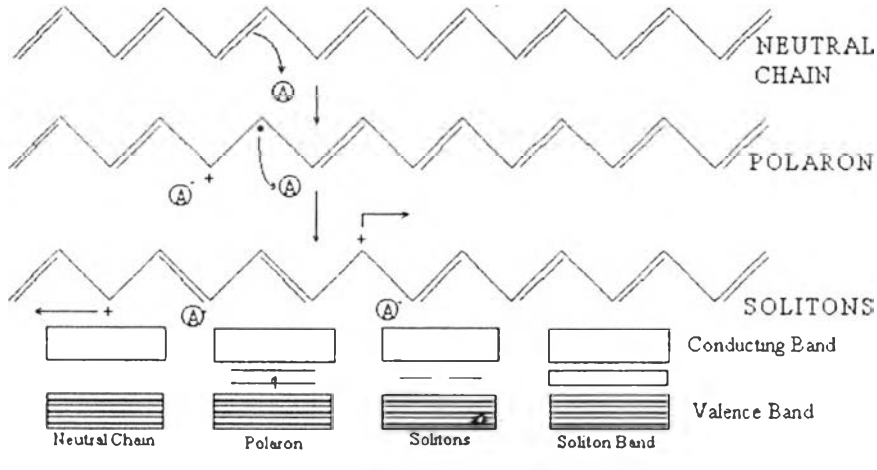


**Figure 2.4** Mechanism of polyacetylene when becomes doped (Pratt, 1996).

**Table 2.2** The physical properties of conductive polymers

| Conductive polymers | Electrical Conductivity (S/cm) | Biocompatibility | Reference |
|---|---|---|---|
| Polyacetylene, (PAc) | $10^3 - 1.7\times10^5$ | × | Balint *et al.*, 1995 |
| Polyaniline, (PANI) | $30 - 2\times10^2$ | √ | |
| Polythiophene, (PTh) | $10 - 10^3$ | √ | |
| Polypyrrole, (PPy) | $10^2 - 7.5\times10^3$ | √ | |
| Poly(3,4-ethylenedioxythiophene), (PEDT, PEDOT) | $10 - 10^3$ | √ | Valle *et al.*, 2007 |
| Poly(p-phenylene), (PPP) | $10^2 - 10^3$ | √ | Balint *et al.*, 1995 |
| Poly(p-phenylenesulfide), (PPS) | $1\times10^2 - 5\times10^2$ | × | Wayne *et al.*, 1976 |
| Poly(p-phenylenevinylene), (PPV) | $3\times10^3 - 5\times10^3$ | × | Balint *et al.*, 1995 |
| Polyfuran, (PFU) | $1 - 10^2$ | √ | Ates, 1995 |
| Polycarbazole, (PCB) | $10^2 - 10^5$ | √ | Ra *et al.*, 2009 |

## 2.4 Polycarbazole (PCB)

Polycarbazole is polymerized from carbazole monomers, which are aromatic heterocyclic organic compound. Carbazole has a tricyclic structure consisting of two six-membered benzene ring fused on either side of a five-membered nitrogen containing ring. Polycarbazole has been employed in several applications, such as light-emitting diodes, electrochromic displays, organic transistors, and rechargeable batteries. The carbazole unit is very interesting for the following reasons (Morin *et al.*, 2007)

1. 9H-carbazole is a very cheap starting material.
2. It is a fully aromatic unit providing a better chemical and environmental stability.
3. The nitrogen atom can be easily substituted with many functional groups helping polymer solubility, optical, and electrical properties.
4. It processes a bridged biphenyl unit resulting in a material with a lower band gap than poly(p-phenylene).

The carbazole unit can be polymerized at the 3- and 6- positions to yield poly(3,6-carbazole) derivatives due to the extreme reactivity of these positions, as well as at the 2- and 7- positions to provide poly(2,7-carbazole) derivatives, with different properties and wide range of the applications (Morin *et al.*, 2007).

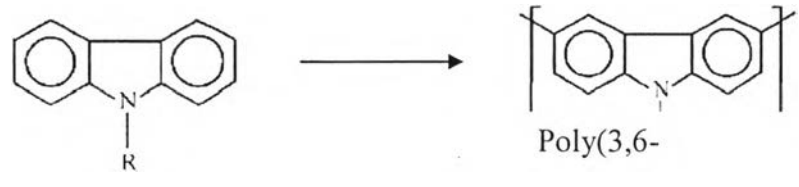


**Figure 2.5** Chemical structure of Poly(3,6-carbazole) and its starting materials.

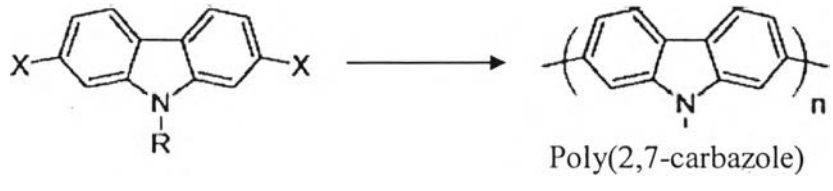


**Figure 2.6** Chemical structure of poly(2,7-carbazole) and its starting materials.

There are two major methods to polymerize polycarbazole which are the chemical polymerization and the electrochemical polymerization. Through the chemical polymerization, monomers react with an excess amount of oxidant in a

suitable solvent. The polymerization takes place spontaneously. Another method is the electrochemical polymerization which involves using of working and reference electrodes, into the solution containing diluted monomer and electrolyte (dopant) in solvent. After applying the voltage, a polymer film immediately forms on the electrode surface in one step. The advantages of chemical route are this synthesis is the most suitable route for the large scale production, it yields a polymer having a higher molecular weight with the possibility to control morphology, and there is no need to get rid of the impurity from the electrochemical polymerization (Harun *et al.*, 2007; Gupta *et al.*, 2010; Raj *et al.*, 2010).

The following literature reviews are about the polymerization of poly(3,6-carbazole) and mechanism of doping process;

Verghese *et al.* (1995) studied the preparation, the electroactivity, the doping/undoping reactions of polycarbazole, and the effect of pH of the medium on the properties of polycarbazole, while emphasizing the similarity of polycarbazole to polyaniline. Polycarbazole film was electrochemically prepared by the potentiostatic oxidation in a $CH_3OH$-$HClO_4$ mixture. The electrochemical oxidation of carbazole, shown in Figure 2.7, produced initially the 3,3'-dicarbazyl radical cation that underwent further oxidation at the same potential and couples to give polymeric products with the elimination of protons. Electrical conductivity of the synthesized polycarbazole yielded values around $10^{-4}$ S/cm. When polycarbazole was treated with ammonia to study the reduction of polycarbazole, it was found that the proton doping and undoping were not easily reversible. Moreover, the pH of the medium influenced the redox behavior of polycarbazole, same as polyaniline. At very low pH values, polycarbazole became highly proronated and amine nitrogen was also protonated. Consequently, at low pH, the availability of a lone pair of elelctrons at nitrogen was reduced. If pH value was greater than 3, the degradation of polycarbazole film occurred.

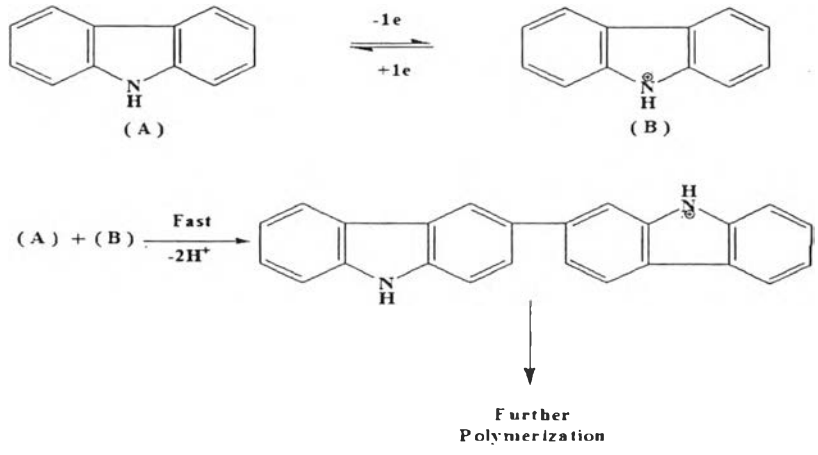


**Figure 2.7** The mechanism of polycarbazole formation (Verghese *et al.*, 1995).

Abthagir *et al.* (1998) studied the time and temperature dependences of conductivity to understand the aging process and the mechanism of conduction. The conductivity of polycarbazole perchlorate was found to be $5\times10^{-4}$ S/cm at the temperature range of 308-450 K. The results showed that the thermal reaction involved with the elimination of dopant, followed by the degradation of the polymer backbone. The conductivity fitted the Arrhenius equation suggesting the nearest-neighbor hopping mechanism.

Taoudi *et al.* (2000) compared the properties and morphology of polycarbazole obtained by the electrochemical polymerization of monomers either in solution or in thin film form by the thermal evaporation on the electrode. The solution used was acetonitrile and water containing tetraethylammonium perchlorate as the electrolyte. The room temperature electrical conductivity obtained from thin film sample was $1.5\times10^{-5}$ S/cm and $5\times10^{-7}$ S/cm in the case of solution sample. The results showed not only polycarbazole thin films obtained by the electrochemical oxidation of vacuum predeposited carbazole monomers films, but also the polymerization efficiency was better than that obtained by the polymerization of carbazole monomers in solution in the electrolyte.

Inzelt (2003) studied the formation and the redox behavior of polycarbazole prepared by electropolymerization of solid carbazole crystals. The results showed that during the polymerization anions and water molecules entered into the surface

layer. However, these species left the film after the reduction of the polymer formed. The redox processes in Figures 2.8 and 2.9 were accompanied by a color change from a pale yellow/colorless (reduced) to a dark green (oxidized) form. The comparison of the mass change and the amount of charge consumed during the reversible redox transformations of the polymer suggested that the oxidation of the polymer involved a mixed cationic and anionic charge transport, i.e. the desorption of $H^+$ ions and the sorption of $ClO_4^-$ ions.

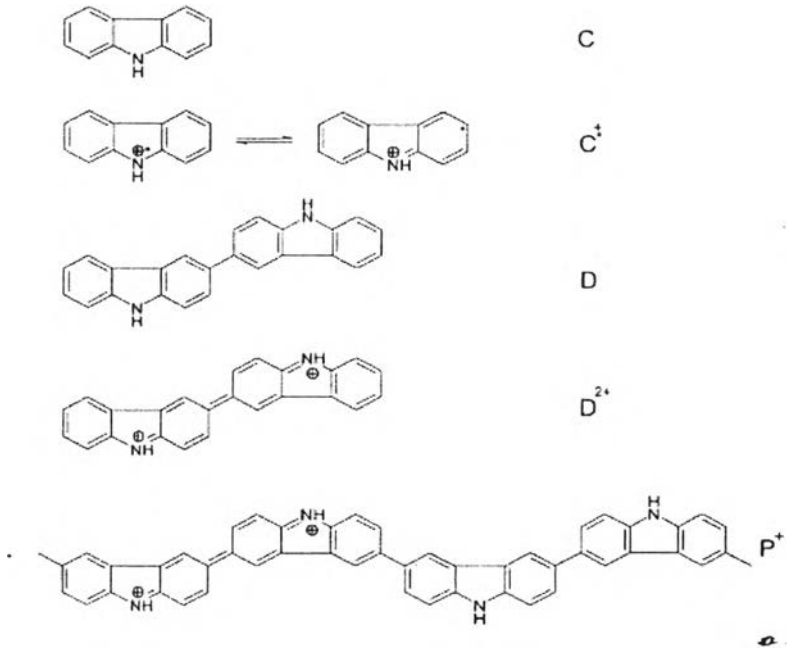


**Figure 2.8** The structure of carbazole (C) and its oxidation products: $C^+$ is cation radical, D and $D^{2+}$ are dimer and dimer dication, respectively, and $P^+$ is the half-oxidized polymer (Inzelt, 2003).

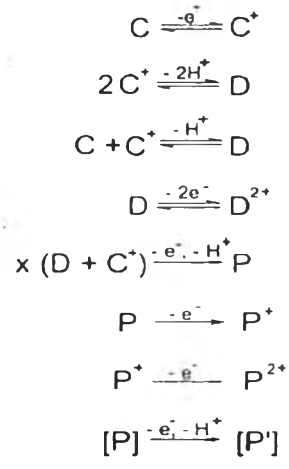

**Figure 2.9** Scheme of the oxidation and demerization of carbazole as well as the redox transformations of the dimer/polymer (Inzelt, 2003).

Siove *et al.* (2004) synthesized a new electroactive well-defined poly(3,6-carbazole), as illustrated in Figure 2.10, with a twisted structure due to steric hindrance of the adjacent 1,4,5,8,9 pentamethylcarbazole with $FeCl_3$ as the oxidizing agent in chloroform solution via the traditional chemical route. They also studied the effect of the amount of $FeCl_3$ on both the polymerization yield and the molecular weight of the soluble polymer fractions. Upon addition of larger excess of $FeCl_3$ proportion, polymer gel increased possibly because of the extra oxidation involving intra-chain coupling via the 2,7 tertiary carbons. Furthermore, the polymerization required theoretically at least two $FeCl_3$ equivalents with respect to monomers. The twisting between consecutive rings arised from the strong steric repulsion between the methyl groups (4, 5) with the hydrogen atoms (2, 7) in ortho-positions from each 3,6 junction.

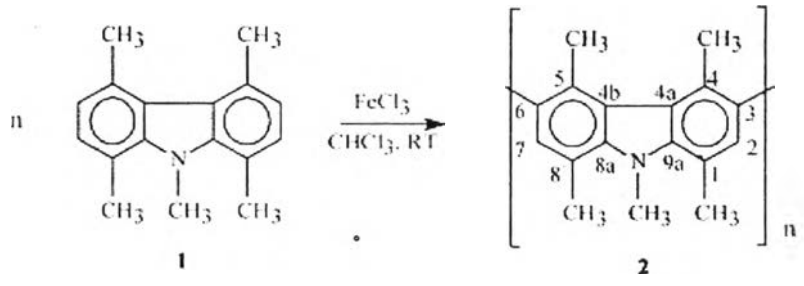


**Figure 2.10** Synthesis of poly(1,4,5,8,9-pentamethyl-3,6-carbazolylene (2) by oxidative polymerization with $FeCl_3$ of pentamethylcarbazole (1) (Siove *et al.*, 2004).

Abthagir *et al.* (2004) prepared polycarbazole electrochemically in a $CH_3OH$-$HClO_4$ mixture and studied the charge transport and their thermal properties. Doped samples of the polymers were obtained by a treatment with 0.1 M ammonium hydroxide for about 6 h. The conductivity of polycarbozole was measured in the temperature range between 306 and 475 K. The result showed that the conductivity gradually increased with increase temperature up to 413 K, where a maximum value of $1.27\times10^{-3}$ S/cm was observed. The nature and the chemical reactivity of the dopant, the process of doping, the doping level, and the polymer crystallinity were found to play a vital role in controlling the conductivity. Thus, the conduction process in polymers was a complex phenomenon.

Macit *et al.* (2004) studied an electroinitiated and a polymerized polycarbazole in acetonitrile using tetrabutylammonium tetrafluoroborate (TBAFB) by the direct electron transfer via the constant potential electrolysis based on an anodic peak potential. It had been observed that polymer yield increased with time, monomer concentration, and polymerization potential. According to the electrochemical polymerization mechanism as shown in Figure 2.11, carbazole was first oxidized at the anode, giving 3,3'-dicarbazyl cation, and the polymerization proceeded in successive steps. When potential was applied, the surface of working electrode was coated with a dark green film, and the solution was converted into a green color, which was indicative of dimer, trimer, and etc. An increase in monomer concentration caused the formation of a higher amount of radical cation and

indirectly caused an increase in the polymerization rate. Also, the electrical conductivities were measured to be about $10^{-3}$-$10^{-4}$ S/cm and increased with decreasing temperature.

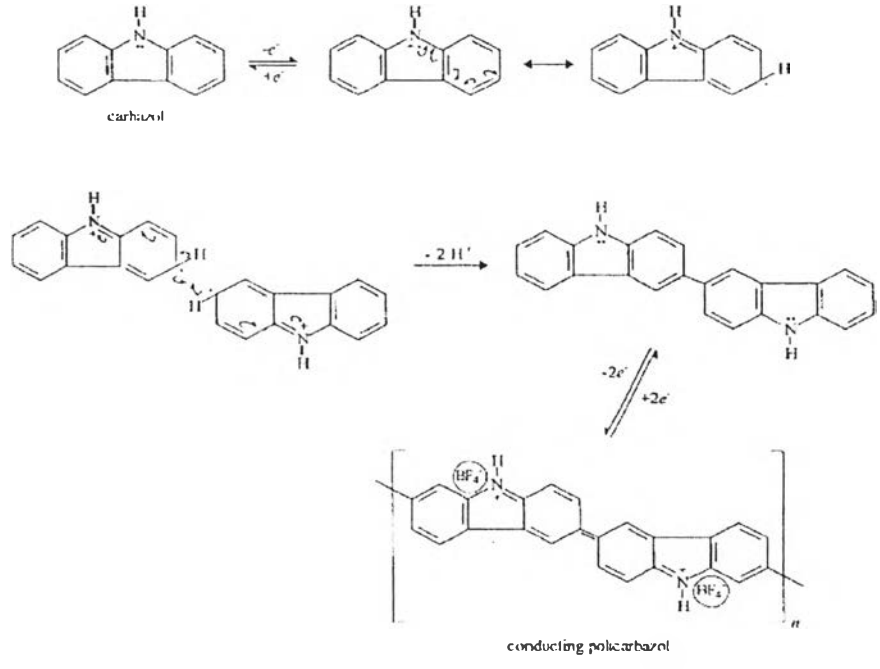


**Figure 2.11** Proposed mechanistic scheme for the electropolymerization of carbazole (Macit *et al.*, 2004).

Zhuang *et al.* (2009) electropolymerized polycarbazole on indium tin oxide (ITO) electrodes in two air- and water-stable room-temperature ionic liquids, 1-butyl-3-methylimidazolium hexafluorophosphate (BMI-$PF_6$) and N-butyl-N-methylpyrrolidinium bis((trifluoromethyl)sulfonyl)imide (BMP-TFSI) using three potentiostatic methods (cyclic votammetry, potentiostatic electrolysis, and potentiostatic pulse electrolysis). The polymer films showed electrochromic behavior. The electrical conductivity of the polycarbazole films obtained from BMP-TFSI was 4.52 ± 0.45 mS/cm, whereas the electrical conductivity of films obtained from BMI-$PF_6$ was 11.5 ± 1.48 mS/cm. It can be concluded that BMI-$PF_6$ was a better solvent for preparing polycarbazole films with high electrical conductivity.

Gupta *et al.* (2010) studied the effect of supporting electrolytes on electropolymerization, redox property, impedance, and crystallinity of polycarbazole. Two different supporting electrolytes tetrabutylammonium perchlorate ($TBAClO_4$) and tetrabutylammonium tetrafluoroborate ($TBABF_4$) dissloved in acetonitrile were used for the synthesis of polycarbazole. The results showed that $TBAClO_4$ was a better supporting electrolyte than $TBABF_4$. Because the compact and dense polymer film obtained from $TBABF_4$ with high crystallinity reduced the diffusion of the ion in and out of the polymer chain, and the electroactivity and conductivity were affected. The conductivity of polycarbazole-$TBAClO_4$ and polycarbazole-$TBABF_4$ were $9.54\times10^{-2}$ and $20.44\times10^{-3}$ S/cm, respectively.

Raj *et al.* (2010) synthesized polycarbazole by the chemical polymerization in acetonitrile medium using ammonium persulfate as an oxidant. The selection of solvents, concentration of the monomer, composition of the solvent, polymerization time, temperature, and pH were optimized to obtain better quality and yield of the polycarbazole. The FT-IR spectra showed that polycarbazole seems to be essentially composed of the recurring carbazole 2,5-diyl unit. The electrical conductivity was maximum at $8.2\times10^{-5}$ S/cm at 65°C. Beyond the temperature of 65°C, the conductivity tended to decrease corresponding to the loss of water molecules.

Gupta *et al.* (2010) polymerized polycarbazole with controlled morphology using the interfacial polymerization. The interfacial polymerization was performed at room temperature using ammonium peroxodisulfate as the oxidant dissolving in HCl. A solution of carbazole monomer in dichloromethane was added in the oxidant solution. Thin films were observed at the interface which later diffused into the non-aqueous phase. The aqueous phase was removed and solid films were collected by filtration washed with water and dichloromethane. Radical cations were formed by the oxidation of the monomers at the micelles near the interface and grown inside the micelles. It had been proposed that the spherical micelles formed in the reaction might be regarded as a soft template in forming hollow spheres.

Bhavana *et al.* (2010) studied one dimensional nanotube and three dimensional hollow spheres of conducting polymers which have attracted immense attention due to their unique properties and potential applications. There are two routes of synthesizing these systems via electrochemical and chemical synthesis.

However, the chemical polymerization has incurred a particular interest because of two major advantages possibility of bulk synthesis and control of morphology. In this article, it was reported for the first time the chemical synthesis of unsubstituted polycarbazole and the formation of its hollow microspheres. Carbazole was polymerized with controlled morphology using interfacial polymerization; however, so far it is known to be possible to synthesize using the electrochemical technique. Upon comparative analysis with polymer synthesized through electrochemical route, it was observed that polymer synthesized through the interfacial polymerization had higher crystallinity with spherical morphology. Formation and growth of microspheres were observed with AFM and SEM micrographs.

## 2.5 Alginate Hydrogel

Alginate is a naturally occurring anionic polymer typically obtained from brown seaweed, and it has been extensively investigated and used for many biomedical applications, due to its biocompatibility, low toxicity, relatively low cost, and mild gelation by addition.

Kuen *et al.* (2012) provided a comprehensive overview of general properties of alginate and its hydrogels, and their biomedical applications.

### 2.5.1 Generation Properties of Alginate

Commercially available alginate is typically extracted from brown algae (Phaeophyceae), including Laminaria hyperborea, Laminaria digitata, Laminaria japonica, Ascophyllum nodosum, and Macrocystis pyrifera by treatment with aqueous alkali solutions, typically with NaOH. The extract is filtered, and either sodium or calcium chloride is added to the filtrate in order to precipitate alginate. This alginate salt can be transformed into alginic acid by treatment with dilute HCl. After further purification and conversion, water-soluble sodium alginate powder is produced. On a dry weight basis, the alginate contents are 22–30% for A. nodosum and 25–44% for L. digitata. (Kuen *et al,* 2012)

Until Fischer and Dörfel identified the l-guluronate residue, and d-mannuronate was regarded as the major component of alginate. Fractional

precipitation with manganese and calcium salts demonstrated later that alginates are actually block copolymers, and that the ratio of guluronate to mannuronate varies depending on the natural source. Alginate is now known to be a whole family of linear copolymers containing blocks of (1,4)-linked β-d-mannuronate (M) and α-l-guluronate (G) residues. The blocks are composed of consecutive G residues (GGGGGG), consecutive M residues (MMMMMM), and alternating Mand G residues (GMGMGM) (Figure 2.12). Alginates extracted from different sources differ in M and G contents as well as the length of each block, and more than 200 different alginates are currently being manufactured. The G-block content of L. hyperborean stems is 60%, and for other commercially available alginates is in the range of 14.0–31.0%.

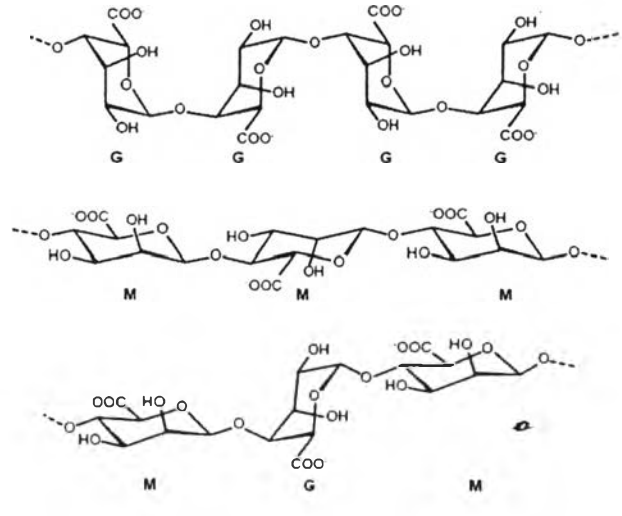


**Figure 2.12** The blocks are composed of consecutive G residues, consecutive M residues, and alternating M and G residues (Kuen *et al*, 2012).

2.5.2 Hydrogel Formation

Alginate is typically used in the form of a hydrogel in biomedicine, including wound healing, drug delivery and tissue engineering applications. Hydrogels are three dimensionally cross-linked networks composed of hydrophilic polymers with high water content. Hydrogels are often biocompatible, as they are

structurally similar to the macromolecular based components in the body, and can often be delivered into the body via minimally invasive administration. Chemical and/or physical crosslinking of hydrophilic polymers are typical approaches to form hydrogels, and their physicochemical properties are highly dependent on the crosslinking type and crosslinking density, in addition to the molecular weight and chemical composition of the polymers (Kuen *et al*, 2012).

*2.5.2.1 Ionic Crosslinking*

The most common method to prepare hydrogels from an aqueous alginate solution is to combine the solution with ionic crosslinking agents, such as divalent cations. The divalent cations are believed to bind solely to guluronate blocks of the alginate chains, as the structure of the guluronate blocks allows a high degree of coordination of the divalent ions. The guluronate blocks of one polymer then form junctions with the guluronate blocks of adjacent polymer chains in what is termed the egg-boxmodel of cross-linking, resulting in a gel structure. Calcium chloride ($CaCl_2$) is one of the most frequently used agents to ionically crosslink alginate. However, it typically leads to rapid and poorly controlled gelation due to its high solubility in aqueous solutions. One approach to slow and control gelation is to utilize a buffer containing phosphate (e.g., sodium hexametaphosphate), as phosphate groups in buffer compete with carboxylate groups of alginate in the reaction with calcium ions, and retard gelation. Calcium sulfate ($CaSO_4$) and calcium carbonate ($CaCO_3$), due to their lower solubilities, can also slow the gelation rate and widen the working time for alginate gels. For example, an alginate solution can be mixed with $CaCO_3$, which is not soluble in water at neutral pH. Glucono-δ-lactone is then added to the alginate/$CaCO_3$ mixture in order to dissociate $Ca^{2+}$ from the $CaCO_3$ by lowering the pH. The released $Ca^{2+}$ subsequently initiates the gelation of the alginate solution in a more gradual manner.

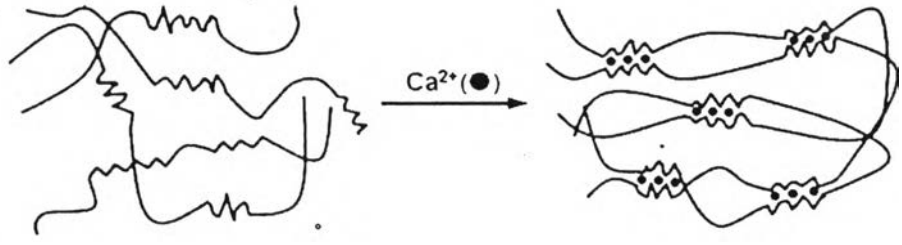


**Figure 2.13** Alginate hydrogels prepared by ionic crosslinking (Kuen *et al*, 2012).

The gelation rate is a critical factor in controlling gel uniformity and strength when using divalent cations, and slower gelation produces more uniform structures and greater mechanical integrity. The gelation temperature also influences gelation rate, and the resultant mechanical properties of the gels. At lower temperatures, the reactivity of ionic crosslinkers (e.g., $Ca^{2+}$) is reduced, and cross-linking becomes slower. The resulting crosslinked network structure has greater order, leading to enhanced mechanical properties. In addition, the mechanical properties of ionically crosslinked alginate gels can vary significantly depending on the chemical structure of alginate. For example, gels prepared from alginate with a high content of G residues exhibit higher stiffness than those with a low amount of G residues.

One critical drawback of ionically crosslinked alginate gels is the limited long term stability in physiological conditions, because these gels can be dissolved due to release of divalent ions into the surrounding media due to exchange reactions with monovalent cations. In addition, the calcium ions released from the gel may promote hemostasis, while the gel serves as a matrix for aggregation of platelets and erythrocytes. These features may be beneficial or negative, depending on the situation, but a desire to avoid these biological reactions, along with more general limitations of ionically crosslinked gels has led to interest in covalently crosslinked alginate hydrogels.

*2.5.2.2 Covalent Crosslinking*

Covalent crosslinking has been widely investigated in an effort to improve the physical properties of gels for many applications, including tissue engineering. The stress applied to an ionically crosslinked alginate gel relaxes

as the cross-links dissociate and reform elsewhere, and water is lost from the gel, leading to plastic deformation. While water migration also occurs in covalently cross-linked gels, leading to stress relaxation, the inability to dissociate and reform bonds leads to significant elastic deformation. However, covalent cross-linking reagents may be toxic, and the unreacted chemicals may need to be removed thoroughly from gels.

Covalent cross-linking of alginate with poly(ethylene glycol)-diamines of various molecular weights was first investigated in order to prepare gels with a wide range of the mechanical properties. While the elastic modulus initially increased gradually with an increase in the crosslinking density or weight fraction of poly(ethylene glycol) (PEG) in the gel, it subsequently decreased when the molecular weight between cross-links ($M_c$) became less than the molecular weight of the softer PEG. It was subsequently demonstrated that the mechanical properties and swelling of alginate hydrogels can be tightly regulated by using different kinds of crosslinking molecules, and by controlling the cross-linking densities. The chemistry of the crosslinking molecules also significantly influenced hydrogel swelling, as would be expected. The introduction of hydrophilic crosslinking molecules as a second macromolecule (e.g. PEG) can compensate for the loss of hydrophilic character of the hydrogel resulting from the crosslinking reaction.

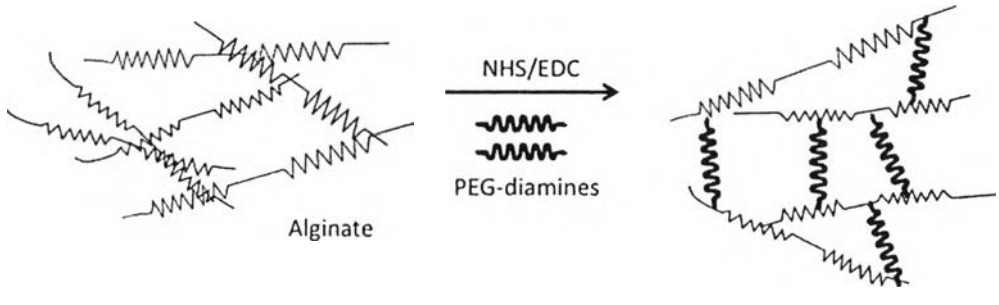


**Figure 2.14** Alginate hydrogels prepared by covalent crosslinking (Bidarra *et al*, 2014).

### 2.5.3 Biomedical Applications

#### *2.5.3.1 Pharmaceutical Applications*

The conventional role of alginate in pharmaceutics includes serving as thickening, gel forming, and stabilizing agents, as alginate can play a significant role in controlled release drug products. Oral dosage forms are currently the most frequent use of alginate in pharmaceutical applications, but the use of alginate hydrogels as depots for tissue localized drug delivery is growing.

Controlled release sodium alginate (Na–Alg) beads containing diclofenac sodium DS have been prepared by precipitation of Na–Alg in alcohol followed by crosslinking with glutaraldehyde (GA) in acidic medium. Preparation of the beads was optimized by considering the percentage entrapment efficiency, swelling capacity of beads in water and their release data. The percentage entrapment efficiency was found to vary between 30 and 71 depending upon the conditions of their preparations. The beads produced at higher temperatures and longer times of exposure to the crosslinking agent have shown the lower entrapment efficiency, but extended release of DS from the beads. The scanning electron microscopic studies indicated nonporous smooth surfaces and the differential scanning calorimetric data indicated the molecular level dispersion of the drugs in the beads. (Anandrao *et al.*, 1999)

Kulkarni *et al.*, 2000 presented experimental results on the successful encapsulation of a natural liquid pesticide "neem seed oil" hereafter designated as NSO, using sodium alginate (Na-Alg) as a controlled release (CR) polymer after crosslinking with glutaraldehyde (GA). The NSO-containing beads have been prepared by changing the experimental variables such as the extent of crosslinking and the amount of loading in order to optimize the process variables. The absence of chemical interactions between active ingredients and polymer as well as crosslinking agent was confirmed by FTIR spectral measurements. The SEM data indicated that the structure of the walls of the beads is smooth and nonporous. The swelling results indicated that swelling of the polymeric beads decreased with increasing exposure time to the crosslinking agent. However, no significant variation in swelling was observed with different amounts of NSO loading. In order to

understand the crosslink ability and its effect on the NSO release patterns of the beads, an attempt was made to calculate the molar mass between crosslinking points using the Flory–Rehner equation. The release data have been fitted to an empirical equation to estimate the kinetic parameters (Kulkarni *et al.*, 2000).

*2.5.3.2 Wound Dressings*

The treatment of acute and chronic wounds is a pressing need in many facets of medicine, and alginate based wound dressings offer many advantageous features. Traditional wound dressings (e.g., gauze) have provided mainly a barrier function keeping the wound dry by allowing evaporation of wound exudates while preventing entry of pathogen into the wound. In contrast, modern dressings (e.g., alginate dressings) provide a moist wound environment and facilitate wound healing. Alginate dressings are typically produced by ionic crosslinking of an alginate solution with calcium ions to form a gel, followed by processing to form freeze dried porous sheets (i.e., foam), and fibrous nonwoven dressings. Alginate dressings in the dry form absorb wound fluid to re-gel, and the gels then can supply water to a dry wound, maintaining a physiologically moist microenvironment and minimizing bacterial infection at the wound site. These functions can also promote granulation tissue formation, rapid epithelialization, and healing.

Sodium alginate (SA) and gelatine (G) based hydrogels with various SA/G ratios, crosslinked with calcium ions ($Ca^{2+}$) and glutaraldehyde (GTA), respectively, were developed. Scanning electron microscopy, Fourier transform infrared spectroscopy (FTIR), and dynamic mechanical analysis (DMA) were applied to determine their physicochemical characterization. The swelling studies, conducted in phosphate buffered saline with a pH ranging from 1 to11 at 371°C, were utilized for an evaluation of their absorption ability. FTIR spectra of the $Ca^{2+}$ crosslinked SA/G hydrogels revealed a small shift in symmetric stretching carboxyl groups, indicating an ionic binding between the $Ca^{2+}$ ions and the SA. Increasing the G content in hydrogels crosslinked with GTA significantly changed the shapes of the amide I and II bands in the FTIR spectra, thus confirming the G–GTA crosslink formation. After crosslinking, a DMA study proved the enhanced viscoelastic properties and improved thermal stability of the prepared samples. The obtained data indicated that $Ca^{2+}$ crosslinked hydrogels with a SA/G 50/50 ratio provided a good

balance of swelling and viscoelastic properties, making them applicable as a potential nontoxic wound dressing material capable of adequately assuring a moist environment, elasticity and mechanical strength for comfortable wound healing. (Saarai *et al.*, 2013)

*2.5.3.3 Cell Culture*

Alginate gels are increasingly being utilized as a model system for mammalian cell culture in biomedical studies. These gels can be readily adapted to serve as either 2-D or more physiologically relevant 3-D culture systems. The lack of mammalian cell receptors for alginate, combined with the low protein adsorption to alginate gels allows these materials to serve in many ways as an ideal blank slate, upon which highly specific and quantitative modes for cell adhesion can be incorporated (e.g., coupling of synthetic peptides specific for cellular adhesion receptors). Further, basic findings uncovered with in vitro studies can be readily translated in vivo, due to the biocompatibility and easy introduction of alginate into the body. (Kuen *et al,* 2012)

Functionalized alginate and poly(ethylene glycol) (PEG) polymers were used to generate covalently linked alginate–PEG (XAl-g-PEG) microbeads of high stability. The cell compatible Staudinger ligation scheme was used to crosslink phosphine terminated PEG chemoselectively to azide-functionalized alginate, resulting in XAlgPEG hydrogels. XAlgPEG microbeads were formed by co-incubation of the two polymers, followed by ionic crosslinking of the alginate using barium ions. The enhanced stability and gel properties of the resulting XAl-g-PEG microbeads, as well as the compatibility of these polymers for the encapsulation of islets and beta cells lines, were investigated. The data showed that XAl-g-PEG microbeads exhibited superior resistance to osmotic swelling compared with traditional barium crosslinked alginate (Ba–Alg) beads, with a five-fold reduction in observed swelling, as well as resistance to dissolution via chelation solution. Diffusion and porosity studies found XAl-g-PEG beads to exhibit properties comparable with standard Ba–Alg. XAl-g-PEG microbeads were found to be highly cell compatible with insulinoma cell lines, as well as rat and human pancreatic islets, where the viability and functional assessment of cells within XAl-g-PEG were comparable with Ba–Alg controls. The remarkable improved stability, as well as

demonstrated cellular compatibility, of XAl-g-PEG hydrogels makes them an appealing option for a wide variety of tissue engineering applications. (Hall *et al*, 2011).

Alginate hydrogels are extremely versatile and adaptable biomaterials, with great potential for use in biomedical applications. Their extracellular matrix-like features have been key factors for their choice as vehicles for cell delivery strategies aimed at tissue regeneration. A variety of strategies to decorate them with biofunctional moieties and to modulate their biophysical properties have been developed recently, which further allow their tailoring to the desired application. Additionally, their potential use as injectable materials offers several advantages over preformed scaffold-based approaches, namely: easy incorporation of therapeutic agents, such as cells, under mild conditions; minimally invasive local delivery; and high contourability, which is essential for filling in irregular defects. Alginate hydrogels have already been explored as cell delivery systems to enhance regeneration in different tissues and organs. Here, the in vitro and in vivo potential of injectable alginate hydrogels to deliver cells in a targeted fashion is reviewed. In each example, the selected crosslinking approach, the cell type, the target tissue and the main findings of the study are highlighted. (Silvia *et al.*, 2014)

*2.5.3.4 Muscle, Nerve, Pancreas, and Liver*

Alginate gels are also being actively investigated for their ability to mediate the regeneration and engineering of a variety of other tissues and organs, including skeletal muscle, nerve, pancreas, and liver. Current strategies for skeletal muscle regeneration include cell transplantation, growth factor delivery, or a combination of both approaches, and alginate gels have found potential in these strategies. A combined delivery of VEGF and insulin-like growth factor-1 (IGF-1) from alginate gels was used to modulate both angiogenesis and myogenesis. The localized and sustained delivery of both growth factors led to significant muscle regeneration and functional muscle formation, due to satellite cell activation and proliferation, and cellular protection from apoptosis by the released factors. Long-term survival and outward migration of primary myoblasts into damaged muscle tissue in vivo from RGD-alginate gels were dramatically enhanced by the sustained delivery of hepatocyte growth factor (HGF) and fibroblast growth factor 2 (FGF 2)

from gels. This led to extensive repopulation of host muscle tissues and increased the regeneration of muscle fibers at the wound site. (Kuen *et al.*, 2012)

Yanyan *et al.* (2012) alginate was crosslinked by a condensation reaction of cystamine or cysteine with diterminated amine groups to form hydrogels containing disulfide bonds. These hydrogels were easily decomposed or disintegrated under physiological reducible conditions by cleavage of disulfide crosslinkage to thiol groups. Porous alginate hydrogel scaffolds were prepared by a freeze drying technique. Results indicated that the pore structure and decomposition properties of the scaffolds were determined by a concentration of alginate solution as well as the amount and types of crosslinker. With surface modification using chitosan, the mechanical properties of the scaffolds were greatly improved. Cytotoxicity evaluation demonstrated that these alginate scaffolds were cytocompatible (Yanyan *et al*, 2012).

## 2.6 Electroactive Conductive Polymer/Bio-Gel Blends

Electroconductive hydrogels (ECHs) are composite biomaterials that bring together the redox switching and electrical properties of inherently conductive electroactive polymers (CEPs) with the facile small molecule transport, high hydration levels and biocompatibility of cross-linked hydrogels.

Pattavarakorn *et al.* (2012) prepared the conductive polythiophene/ chitosan/carboxymethylchitosan (PTH/CS/CMCS) hydrogel. Polythiophene was synthesized via oxidative polymerization in chloroform at 40°C. For CMCS synthesis, CS was alkalized with sodium hydroxide in isopropanol and then reacted with monochloroacetic acid at 50°C. The synthesized PTh and CMCS were mixed with CS by solution blending, glutaraldehyde crosslink agent was added and then the conductive hydrogel films were casted. The effects of CS/CMCS ratio, glutaraldehyde concentration, electric field strength and PTh particle addition on conductivehydrogel properties; morphology, crystallinity, thermal stability, tensile strength and electroactive performances were investigated. The results show that the CS/CMCS hydrogel responded well to an applied DC electric field by bending towards an electrode, in which the bending angle increased with the increase of

electric field strength. The crosslinked CS/CMCS hydrogel showed better response than uncrosslinked hydrogel. Moreover, the conductive PTh/CS/CMCS hydrogel showed lower electroactive performances than the CS/CMCS due to its higher weight and rigidity.

Ismail *et al.* (2011) studied the linear artificial muscles of hydrogel microfibers coated with a conducting polymer as a sensor of driving current, electrolyte concentration and temperature. Hybrid conducting polymer/hydrogel microfibers were fabricated from a chitosan solution through wet spinning technique followed by in situ chemical polymerization of pyrrole in aqueous medium using bis(triflouro methane sulfonyl) imide as dopant. The hybrid microfiber was characterized by FTIR, electrical conductivity measurement, scanning electron microscopy, dynamic mechanical analysis, cyclic voltammetry and chrono-potentiometry. The fiber showed an electrical conductivity of $3.1\times10^{-1}$ S/cm. The electroactivity was impacted by polypyrrole. An electrochemical linear actuation strain of 0.54% was achieved in aqueous electrolyte. The electrochemical measurements were performed as a function of applied current, temperature and concentration for a constant charge in 1 M NaCl. The chrono-potentiometric responses during the oxidation/reduction processes and the resulting linear fit of consumed electrical energy during reaction of the hybrid microfiber for different anodic/cathodic currents and at different temperatures showed that it was a sensor of applied current and temperature, respectively. A logarithmic dependence of the consumed electrical energy with concentration of the electrolyte during reaction suggested that it can act as a concentration sensor.